Observation on dominance of swells over wind-seas in the coastal waters of Gulf of Mannar, India

M. M. Amrutha and V. Sanil Kumar

Ocean Engineering Division, CSIR-National Institute of Oceanography, Dona Paula, Goa 403 004 India

Correspondence to: Sanil Kumar (sanil@nio.org)

Abstract. Wind-seas typically dominate over swell seas in coastal regions of the gulfs. Waves measured at a location having a water depth of 12 m in the nearshore waters of Gulf of Mannar during one year period (1 May 2015 to 30 April 2016) are used to examine the predominance of wind-seas and swells through spectral characterisation. The study shows that even though the location is in a gulf, the annual average value (~0.84 m) of the significant wave height at this area is comparable to that along the coastal waters of the Indian subcontinent, but the annual maximum value (~1.7 m) recorded is much less than that (3 to 5 m) observed in those regions. Also, large seasonal variations are not observed in the wave height. The waves of the study region are under the control of sea-breeze with the maximum in the late evening hours and the minimum in the early morning hours. A 5% increase in the forcing wind field during the monsoon period improved the comparison statistics between the model wave height and the measured values. 53% of the surface height variance in the study area is a result of southeast and south swells and the remaining are the east and southeast wind-seas.

1 Introduction

The Gulf of Mannar (GoM) connects the Arabian Sea in the south to the Palk Bay in the north. Palk Bay is a shallow basin with a maximum water depth of ~13 m and connects to the Bay of Bengal at its northeastern end (Fig. 1). The western region of the GoM is a Marine Biosphere Reserve and slight changes in the waves and meteorological parameters will have large impacts in this area. The seasonal reversal of the monsoon winds in the North Indian Ocean (Wyrtki, 1971) induces changes in the directionality of the surface waves (Sanil Kumar et al., 2012). The winds are from the southwest in the Indian summer monsoon which lasts from June to September and from the northeast during October to January (winter monsoon). As over the rest of India, the winds in the GoM too reverse with the season (Fig.

2). Winds over the region are much stronger in the summer monsoon (~5-7 m s^{-1}) than that during the winter monsoon (~3-5 m s^{-1}). Over this region, the winds during February-May is weak with a seasonal average value less than 3 m s^{-1}.

Arena and Guedes Soares (2009) grouped the sea states with bimodal spectra in 3 sets, i.e., swell dominated seas; wind-sea dominated seas and mixed-seas based on the ratio of the significant wave height of the swells and the wind-seas. Generally, the swells propagating from distant storms and the local wind-seas comprise the waves in the open ocean (Hanson and Phillips, 1999). Mixed-seas are generally observed in coastal regions, bays and gulfs with a dominance of wind-seas regime (Hwang et al., 2011). When the spectrum is bimodal, the wind-seas and the swells can have different directions and it can alter the direction of the littoral drift. The high-frequency wave components govern the momentum flux between the ocean and atmosphere (Cavaleri et al., 2012). The long-period waves cause problems to navigation, offshore operations and induce large motion on the moorings (McComb et al., 2009) and hence, it is necessary to know the occurrence of long-period waves at a location. Recently many studies identified long-period waves in the eastern Arabian Sea (Sanil Kumar et al., 2012; Glejin et al., 2016; Amrutha et al., 2017). Sanil Kumar et al. (2003) observed that in the Indian waters, annually the wave energy spectra contain multiple peaks for about 60% of the time and when the significant wave height (H_{m0}) is higher than 2 m, they are generally single-peaked. The multi-peaked wave spectra observed in the coastal region of India are largely dominated by swells (Sanil Kumar et al., 2003). Most of the studies in the Indian waters are in the eastern Arabian Sea (Sanil Kumar et al., 2003; Sanil Kumar et al., 2012; Glejin et al., 2016; Amrutha et al., 2017; Nair and Sanil Kumar, 2017) and the western Bay of Bengal (Sundar, 1986; Nayak et al., 2013; Patra and Bhaskaran, 2016). The studies on waves in Indian waters based on measured wave data covering 1 year and above are presented in Table 1. Based on one-year measured data, Gowthaman et al. (2013) observed that swells are dominant in the northern GoM from January to April and the wind-sea dominates in the remaining period of the year. Owing to the lack of measurements, our knowledge of the wave characteristics in the western part of the GoM is poor. Hence, in this paper, we describe the wave characteristics based on one year long measured wave data in the western GoM. Apart from describing the seasonal variations, the present study identifies the predominant wave systems in the western GoM. The inter-annual variation in wind-sea and swell percentage in the surface variance based on numerical model results is studied at 8 N; 78.25 E along with the change in wind-sea and swell percentage during one year along the longitude 78.25^{o} E when the waves approach from 7^{o} N to 8.5^{o} N in the GoM are also examined.

The paper is structured as follows. In Section 2 , the data used in the study and the details of numerical model and validation are described. Section 3 is the results part. First, wave parameter statistics are introduced for subsequent use. Second, wave spectral characteristics are presented. Third, the inter-annual variations are presented based on model data and the results are discussed. The summary of the study is given in Section 4.

2 Data and methods

2.1 Data

This study uses measured waves in the western GoM at a location (latitude 8° 52' 52" N; longitude 78° 17' 44" E) having a water depth of 12 m from 1 May 2015 to 30 April 2016. The wave data are recorded in a moored directional waverider buoy continuously at 1.28 Hz for one year period. Heave is measured with 1 cm resolution and with 3% accuracy. A moored wave buoy may travel around a large crest in a short-crested sea, or even be dragged through a large crest if it reaches the limit of its mooring line (Whittaker et al.,2016). Additionally, the Lagrangian buoy motion will still affect the wave measurements of an idealised buoy capable of perfectly following the free surface motions. Although the linear contributions to the free surface elevation measured by a surface-following and fixed sensor are equal, it is generally assumed that this Lagrangian motion will prevent the buoy from measuring the second harmonic component of steep deep-water waves obvious on a wave staff record (Longuet-Higgins, 1986). These effects are not considered in the present study. The wave spectrum is estimated from the measured buoy heave data through a fast Fourier transform of 8 series, each consisting of 256 data points. The resolution of the wave spectrum is 0.005 Hz from 0.025 Hz to 0.1 Hz and thereafter it is 0.01 Hz up to 0.58 Hz. From the wave spectrum, significant wave height (H_{m0}), mean wave period (T_{m02}) and spectral peak period (Tp) are estimated for data covering 30 minutes and the wave direction is obtained based on circular moments (Kuik et al., 1988). Other parameters estimated are the maximum spectral energy density, spectral peakedness parameter (Qp) (Goda, 1970) and spectral narrowness parameter (ν). The directional spectra are based on the Maximum Entropy Method (Lygre and Krogstad, 1986). Measurements reported in this article are in Coordinated Universal Time (UTC) and the local time is 5:30 h ahead of UTC. The method proposed by Portilla et al. (2009) is used to separate the wind-seas and swells from the measured data. The 1-D separation algorithm is on the assumption that, the energy at the peak frequency of a

swell cannot be higher than the value of a Pierson-Moskowitz (PM) spectrum at the same frequency. The ratio between the peak energy of a wave system and the energy of a PM spectrum at the same frequency is above a threshold value of 1, the system is considered to represent wind-sea, else it is taken to be swell and a separation frequency f_c is estimated. Swell and wind-sea parameters are obtained for frequencies ranging from 0.025 Hz to f_c and from f_c to 0.58 Hz, respectively. The deep water (8.27^o N, 78.56^o E) wave data during 1 January to 31 December 2006 is used for comparison of the model results in the deep water.

2.2 Model

Third-generation spectral wave model WAVEWATCH III version 4.18 (Tolman, 1991) is used in the wave hindcast studies. The source term of the model consists of several parts, a wind-wave interaction, nonlinear wave-wave interactions, a dissipation (whitecapping) and wave-bottom interactions. The treatment of the nonlinear interactions defines a third-generation wave model which is modelled here using the discrete interaction approximation (DIA, Hasselmann et al., 1985). The source term package (ST4) of Ardhuin et al. (2010) is used as the input and dissipation source terms. JONSWAP parameterization (BT1) is used as the empirical relation for bottom friction. For the Southern and large part of Indian Ocean domain, the model grid resolution is 0.5^o x 0.5^o (20^o E -112^o E and 70^o S-35^o N) and is 0.1^o x 0.1^o for the North Indian Ocean (65^o E-90^o E and 5^o N - 25^o N). The model is forced with ERA-Interim (Dee et al., 2011) surface wind fields at every 6 h interval with a spatial resolution of 0.5^o. The resolution in wave direction is at 10^o and the wave frequencies are on a logarithmic scale from 0.04 to 0.5 Hz. The model output for the period 1 May 2015 to 30 April 2016 at 4 locations along the longitude 78.25^o E is used to study the variations in the swell percentage when the waves approach from 7^o N to 8.5^o N. The model results (H_{m0}, mean wave period and mean wave direction) are also compared with the ECMWF wave data at longitude 78.25^o E and latitudes 7^o, 7.5^o, 8^o N. Wind-sea and swell percentage from the model output extracted at 8^o N is used for studying the trend in the H_{m0} and the wind-sea and swell percentage for 36 years (1980- 2015). The trend is estimated based on the slope of the linear best-fit curve to the annual mean value for 36 years.

2.3 Error estimates

The error statistics for significant wave height, mean wave period, mean wave direction from the model against measured and ERA-Interim data were computed based on bias, root-mean-square error (rmse), scatter index (SI), and Pearson's linear correlation coefficient (r) as defined below.

$$\text{bias} = \frac{1}{N}\sum_{i=1}^{N}(A_i - B_i) \quad (1)$$

$$\text{rmse} = \sqrt{\frac{1}{N}\sum_{i=1}^{N}(A_i - B_i)^2} \quad (2)$$

$$\text{SI} = \frac{\text{rmse}}{\overline{B}} \quad (3)$$

$$r = \frac{\sum_{i=1}^{N}\left|(A_i - \overline{A})(B_i - \overline{B})\right|}{\sqrt{\sum_{i=1}^{N}\left|(A_i - \overline{A})^2 (B_i - \overline{B})^2\right|}} \quad (4)$$

Where Ai and Bi represent the parameter based on numerical model and measured, N is the number of data points and the over bar represents the mean value.

2.4 Comparison of model output with measured data

The H_{m0} is extracted for the point 8.27° N, 78.56° E from the model and compared with the measured buoy data (Fig. 3). The comparison between model and measured H_{m0} for the year 2006 shows a bias, rmse, SI, r values of -0.18 m, 0.31 m, 0.19 and 0.89 respectively. The wave heights are under predicted by the model and the under prediction is larger during the monsoon period. A 5% increase in the forcing wind field during monsoon period improved the comparison statistics of bias, rmse, SI, r values to -0.10 m, 0.26 m, 0.16 and 0.90 respectively.

We compared the model H_{m0}, mean wave period and mean wave direction with ERA-Interim wave data for three deep water points having the same longitude 78.25° E and different latitudes of 7.0°, 7.5°, 8.0° N (Fig. 4). It is found that the model H_{m0} is comparatively

in good agreement with ERA-Interim H_{m0} with bias ranging from -0.17m to -0.06 m shows the under estimation by the model, rmse is having a range of 0.16 m to 0.17 m, SI ranges from 0.10 to 0.14 and correlation coefficients is around 0.97. The statistical parameters bias, rmse, SI, r for the wave period is having a range of 0.84s to 0.85s, 1.3s to 1.4s, 0.2, 0.84 to 0.85. Similarly, ranges for bias, rmse, SI for mean wave direction are -5.1° to -0.6°, 13.9° to 16.3°, 0.1 respectively.

3 Result and discussions

3.1 Wave parameters statistics

Based on the maxima, mean value and standard deviation, the statistical analysis of the main wave characteristics is obtained. The directional wave parameter presented here is the mean direction corresponding to the spectral peak. The annual maximum H_{m0} measured is 1.70 m and the mean value is 0.84 m (Table 2), whereas H_{m0} less than 0.34 m did not occur over the annual period. The monthly mean H_{m0} varied from 0.7 m in November to 1.08 m in June with a standard deviation of 0.12 m. Slightly higher monthly means of H_{m0} occurred during months from May to September, when means of 0.88 to 1.08 m are observed (Table 2). The lowest values occurred during months from November to April. Variation in monthly average H_{m0} in a year is small (< 0.4 m) in the study area, which is in contrast to the large variations (~2 m) in monthly average values observed in the eastern Arabian Sea (Sanil Kumar et al., 2014). The seasonal variations in the wave height along the Indian coast have been well characterized and show a summer-winter pattern (Sanil Kumar et al., 2012). In the study area, seasonal mean H_{m0} is 0.97, 0.75 and 0.80 m during the summer, winter and fair-weather period (February-May) indicating that large seasonal variations are not observed in H_{m0}. The variation in wave height follows that of the local wind speed. Only during 20% of the time in a year, H_{m0} exceeded 1 m and no maximum wave height (H_{max}) more than 2.9 m was measured at this location. The Sri Lankan land mass is at a distance of 170 km in the northeast direction and 185 km in the southeast direction from the wave buoy location. In the N-NE direction, the Rameshwaram Island is present at a distance of 110 km. The study area is exposed to the Indian Ocean swells from south and southwest. Hence, the wave field at the study location is partially restricted and high waves are not observed compared to that in the open sea conditions along the western Bay of Bengal and the eastern Arabian Sea. Even though the study location is in a Gulf and high waves are not observed, the annual mean H_{m0}

observed at the study region (0.84 m) is comparable to the values (0.7 to 1.1 m) reported for other locations in the western Bay of Bengal and eastern Arabian Sea (Gowthaman et al., 2013; Sanil Kumar et al., 2013).

On 8 November 2015, a depression was formed in the Bay of Bengal and later it was upgraded to a deep depression and crossed the coast of Tamil Nadu near Puducherry with peak wind speeds of 15.3 m s^{-1} (55 km h^{-1}) and a minimum central pressure of 991 hPa (IMD, 2015). Even though the wave measurement location is only 370 km from the track of the depression, the influence of this deep depression is not observed in the measured wave data. This shows that the waves in GoM are not influenced by the storms north of Palk Bay. The gradual increase in wave height seen in May and June is associated with the summer monsoon (Fig. 5). The locally generated waves (wind-sea) and the swells are separated to identify different wave components at the study location. Swell H_{m0} up to 1.23 m are recorded with a mean value of 0.58 m, whereas the mean wind-sea H_{m0} is 0.56 m with a maximum value of 1.62 m. The high wind-sea H_{m0} is observed in May with negligible swell (8-10%) on that occasion; the swell was not always negligible in May.

Wide range (3 to 22 s) is observed in the peak wave period with a mean value of 12 s indicating that the wave regime of the study area consists of short to long period waves. Even though wind-seas and swells are present in the study area, the variation over an annual cycle in mean wave period is 3 to 11 s with the mean value of 4.7 s. For all months, the mean wave periods are still short relative to other areas in the western part of the Bay of Bengal and the eastern part of the Arabian Sea (5 to 6.5 s). Distribution of mean wave direction for the 3 seasons shows that the distribution is similar for the swells throughout the year except in the southwest monsoon months. However, for the wind-seas large variation in wave direction is observed from October to May. Short-period waves (T_p < 6 s) approach from east, northeast, southeast and south except in the southwest monsoon months. In the southwest monsoon period, the short-period waves are from southeast and south. Waves with period more than 8 s are mainly from south and southeast (Fig. 6). Over an annual cycle, 31.6% of the time, long-period waves (T_p>14 s) are also observed (Table 3) and these swell waves are produced from storms in the Southern Ocean and reach the Indian coast within 5 to 6 days (Amrutha et al., 2017).

53% of the surface height variance at the study area over the annual cycle is a result of the south and southeast swells and the balance is the east and southeast wind-seas (Table 2). The wave field at the study region shows the dominance of swells over the wind-seas, which is in agreement with that reported for the areas around the Indian coast (Sanil Kumar et

al., 2003; Sanil Kumar et al., 2012; Glejin et al., 2013; Sanil Kumar et al., 2014). But in the southwest monsoon period, the seasonal average swell contribution is 61%, whereas it varies from 70 to 79% for locations around India (Sanil Kumar et al., 2014). Over the western GoM during most of the time, the wave climate is characterized by sea–land breeze structure and is feeble during November and December (Fig. 7). The waves in the western GoM is under the control of wind–sea generated by sea-breeze in a diurnal pattern with the maximum during the late evening and the minimum during the early morning and is similar to that reported over the south-western Bay of Bengal (Glejin et al., 2013).

Wave length linked with the mean wave period ranged from 14 to 107 m and the ratio of water depth and wave length (varied from 0.11 to 0.85) is more than 0.5 during 27% of the time indicating that for 27% of the time the measured waves are in the deep water condition (USACE, 1984). On separating the waves into wind-sea and swells, it is observed that 97% of the wind-sea are in the deep water condition, whereas 98% of the time, the swells satisfies the transitional water condition. The water depth to wave length ratio shows that the wave height and the wave direction presented in this article will be influenced by the sea bed. Wind and wave direction corresponding to spectral peak differ by 20 to 120° during most of the time since the measurements are made close (~12 km) to the coast and the wave direction will be mostly aligned to the depth contour due to refraction, whereas such changes in wind direction are not expected (Fig. 5). When the difference between the wind and wave direction is more than 45°, the relative water depth based on spectral peak period (d/L_p) shows that the wave regime is in intermediate and shallow water (Fig. 8). During the deep water regime, the difference between the wind and wave direction is less than 45°.

The wind is predominantly southwesterly from March to September and from northeast during October to February and the average wind speed is 4.8 m s^{-1} (Figs. 5a and 5c). The nature of sea state can be recognized based on the wave age (C/U_{10}) and the steepness of wave (H_{m0}/L), where C is the phase speed corresponding to the mean wave period. Based on wave steepness, Thompson et al. (1984) grouped ocean waves as locally generated waves, if the steepness values are greater than 0.025. The wave measurements in this study show that 61% of the time wave steepness is greater than 0.025. An old sea is defined when wave age > 25 and when the wave age < 10, it is a young sea. For the present data, wave age is less than 10 during 98% of the time indicating young-seas with the presence of young-swells. Donelan et al. (1993) identified that the value of the spectrum at full development corresponds to U_{10}/Cp =0.83, where the spectral components above this value

are classified as wind-seas and that below as swells and Cp is the phase speed of the waves corresponding to the spectral peak. For the study location, the inverse wave age is more than 0.83 for 7% of the time (Fig. 9). Inverse wave age values are biased towards lower values with peaks in the range of 0.4-0.8, indicating a young-swell driven wave regime along the study area.

We have examined the variations in swell and wind-sea of the surface height variance as the wave propagates from deep water to the shallow waters based on wave model results. The monthly average swell and wind-sea percentage along a longitude transect of 78.25° E at 7.0°, 7.5°, 8.0° and 8.5° N latitude is presented in Figure 10. The study shows that in all the months, the percentage of swells decreased as the waves moved from open ocean to Bay (7.0° to 8.5° N latitude) with an average decrease of ~5% in the swells, except in August. The linear trend of the wind-sea and swell percentage at 8.0° N; 78.25° E during 1980-2015 shows that the trend is slightly positive (0.05%) for wind-sea and negative (0.05%) for the swells (Fig. 11b). The H_{m0} shows a negligible upward trend (2 cm y^{-}) during 1980-2015 (Fig. 11a). Even though the study area is in a gulf region, since its opening is exactly toward the southwest, the upward trend in H_{m0} observed is due to the increase in wave heights in the Southern Ocean (Hemer et al., 2010). Young et al. (2011) based on the 23 year period (1985-2008) satellite altimeter measurements indicate a weak increase (0-0.25% of annual mean value) of H_{m0} in the north Indian Ocean.

The nonlinearity in the surface elevations are reflected in the sharpening of the wave crests and the flattening of the wave troughs and these effects are reflected in the skewness of the sea surface elevation (Toffoli, 2006). The positive skewness value indicates that the wave crests are bigger than the troughs and zero skewness indicates linear sea states (Anjali Nair and Sanil Kumar, 2017). Figure 12 shows the variation of skewness with significant wave height, mean wave period and mean wave direction. The waves from the east are mainly the wind-seas and gave low skewness values. The high skewness values are for long-period swells (Tp > 16 s) superimposed on the wind-seas. The increase in nonlinearity with the increase in the H_{m0} is not predominant at this location (Figures 12a to 12c). The abnormality index (H_{max}/H_{m0}) more than 2 is observed during 8.5% of the time, but it is only 1.5% for waves with H_{m0} more than 1 m (Fig. 5d).

3.2 Wave spectra

In order to have a better understanding of the wave systems in the study area, we show the characterization of waves through the analysis of each individual spectrum. The wave spectra are generally classified as exhibiting either one or two peaks (Henrique et al., 2015). The dominance of wind-sea or swell systems varied for both cases and are presented in this section. Measured data consists of single-peaked wind-sea, single-peaked swell and wind-sea or swell dominated multi-peaked spectra (Table 4). A majority of the data recorded are multi-peaked spectra (58.5% of the time) and the multi-peaked spectra are swell dominated during 45.3% of time and wind-sea dominated during 12.7% of the time. The peak frequency, (f_p) is shown to be unstable when swell and wind-sea peak energies are similar. The single-peak spectra are mainly swell dominated. Gowthaman et al. (2013) observed that in the northern GoM, swells are predominant in GoM during non-monsoon period (January–April) and during rest of the year wind sea dominates. The multi-peaked spectra observed at the present study area is slightly higher than that (37 to 54%) reported along the eastern Arabian Sea (Sanil Kumar et al., 2014).

The energy distribution of waves over a range of frequencies with time is studied by plotting the normalised wave spectral energy density in the time-frequency frame. Each wave spectrum is normalized by the maximum wave spectral energy density of the respective spectrum. Normalized spectral energy density plots in the time-frequency field indicate the predominance of spectral energy in frequency bands 0.06-0.09 Hz (corresponding to swells) during most of the time except from November to March during which the energy is in 0.18-0.24 Hz (corresponding to wind-seas) in most of the time (Fig. 13). The monthly average wave spectrum shows that the wave spectrum is swell dominated in all the months except in December and January during which the wind-seas dominate (Fig. 14). The peak of the swell part of the monthly averaged wave spectrum varied from 0.07 to 0.08 Hz. Gowthaman et al. (2013) observed dominance of swells are maximum (98%) during March and dominance of wind sea is maximum (94%) during October in the northern GoM.

Waves of different frequency have different directions. Long-period swells (Tp > 14 s) and the intermediate-period waves (14 >Tp> 6 s) are from 150 to 180°, whereas the wind-sea direction varies from southwest to northeast (Fig. 13). Waves with the period less than 4 s are from the northeast and east during November-March and from south-southwest during the remaining period (Fig. 14b). Monthly average wave spectrum has a similar direction for the region from 0.06 to 0.13 Hz in all months, whereas the average monthly direction varies

significantly for regions beyond this frequency range (Fig. 14b). For e.g., waves with the period less than 3 s are from the northeast during December-February, southwest during June-August and southeast during the remaining period. The monthly mean directional wave spectrum shows the spread of spectral energy in different frequencies and direction (Fig. 15). Two well separated peaks in spectral energy are observed from November to April, when the winter monsoon is active.

The wave spectra grouped into different frequency ranges show that the peak frequency of a large number of wave spectra (~ 75%) falls between 0.06 and 0.1 Hz with an average H_{m0} of 0.82 m. The mean wave spectra for different peak frequency range shows that for all groups, double-peaked wave spectra is observed (Fig. 16). The intensity of the secondary peak increased as the spectral peak frequency shifted from a low to a high frequency. The relative distance between the two peaks of the wave spectrum represented by the quotient between the mean wave period of the swell components and the mean period of the wind-sea part varied from 1.9 to 5.8 with a mean value of 3.6 and the larger values indicate more distance between the 2 peaks of the spectrum. During the study period, the spectral narrowness parameter (ν) has an average value of ~0.64 and is marginally higher (~ 0.7 to 0.9) when a multi-modal wave spectrum consisting of high-frequency local waves and the swells from the south Indian Ocean are present. The values of the spectral peakedness parameter ranged between 2 and 3 for high waves and most of the time, spectral peakedness parameter tends to be smaller since the spectral energy is distributed across the swell band.

4 Concluding remarks

One-year measured records of wave show that the waves are lower in the western Gulf of Mannar than in the eastern Arabian Sea and the variation in the wave height in different seasons is also less in the study area. 53% of the surface height variance in the study area is a result of the swells from the south and southeast and the balance is the wind-seas from east and southeast. The seasonal average swell contribution is less than that observed for other locations around India. A majority of the time multi-peaked spectra (58.5% of the time) are observed. Even though the study area is in a gulf region, since its opening is exactly toward the southwest and the winds are also blowing from the southwest during the summer monsoon, the monthly mean wave spectrum is swell dominated in all the months with the exception of December and January during which the wind-seas dominate. The percentage of swells in the surface variance decreased as the waves moved from open ocean to Bay (7° to

8.5° N latitude) in all the months except in August. Over an annual cycle, 31.6% of the time, long-period waves (T_p>14 s) are observed. Wave age of the recorded data is less than 10 during 98% of the time signifying that the measured waves are the young sea mixed with the swells. The increase in nonlinearity with the increase in significant wave height is not prominent at this location. During 1980-2015, the significant wave height shows a negligible upward trend (2 cm y^{-}).

Acknowledgments

Authors thankfully acknowledge the CSIR, New Delhi for facilitating the research work and MoES, New Delhi for the partial financial support given for this research. We thank TM Balakrishnan Nair, A Nherakkol, Jeyakumar, INCOIS for the help. Dr. J. Mohanraj, Professor, Kamaraj College, Tuticorin provided the logistics during data collection and the deployment of the buoy. The deep water wave data used for comparison of the model results are provided by National Institute of Ocean Technology, Chennai. We thank the editor Dr. John M. Huthnance and the two reviewers for the critical comments and suggestions which improved the contents of the paper. This work contributes part of the Ph.D. work of the first author. The authors acknowledge the high performance computing resources made available at CSIR-NIO for conducting the research reported in this paper. This work has NIO contribution No. 2017.

References

Amrutha, M.M., Sanil Kumar, V., and Jesbin George: Observations of long-period waves in the nearshore waters of central west coast of India during the fall inter-monsoon period, Ocean Engineering, 131, 244-262, 10.1016/j.oceaneng.2017.01.014, 2017.

Anjali Nair, M., and Sanil Kumar, V.: Wave spectral shapes in the coastal waters based on measured data off Karwar on the west coast of India, Ocean Science, 13, 365–378, doi:10.5194/os-13-365-2017, 2017.

Ardhuin, F., Rogers, E., Babanin, A. V., Filipot, J. F., Magne, R., Roland, A., van der Westhuysen, A., Queffeulou, P., Lefevre, J. M., Aouf, L., and Collard, F.: Semiempirical dissipation source functions for ocean waves. Part I: Definition, calibration, and validation, J. Phys. Oceanogr., 40, 1917–1941, 2010.

Arena, F., and Guedes Soares, C.: Nonlinear high wave groups in bimodal sea states, J. Waterway, Port, Coastal and Ocean Eng., 135, 69-79, 2009.

Cavaleri, L., Fox-Kemper, B., and Hemer, M.: Wind-waves in the coupled climate system, Bull. Am. Meteorol. Soc., 93, 1651–1661, 2012.

Dee, D. P., Uppala, S. M., Simmons, A. J., Berrisford, P., Poli, P., Kobayashi, S., Andrae, U., Balmaseda, M. A., Balsamo, G., Bauer, P., Bechtold, P., Beljaars, A. C. M., van de Berg, L., Bidlot, J., Bormann, N., Delsol, C., Dragani, R., Fuentes, M., Geer, A. J., Haimberger, L., Healy, S. B., Hersbach, H., Hólm, E. V., Isaksen, L., Kållberg, P., Köhler, M., Matricardi, M., McNally, A. P., Monge-Sanz, B. M., Morcrette, J.-J., Park, B.-K., Peubey, C., de Rosnay, P., Tavolato, C., Thépaut, J.-N., and Vitart, F.: The ERA-Interim reanalysis: Configuration and performance of the data assimilation system, Q. J. Roy. Meteor. Soc., 137, 553–597, 2011.

Donelan, M. A., Dobsen, F. W., Smith, S. D., and Anderson, R. J: On the dependence of sea surface roughness on wave development. J**.** Phys**.** Oceanogr**.,** 23, 2143–2149, 1993.

Glejin, J., Sanil Kumar, V., Amrutha, M. M., and Singh, J.: Characteristics of long-period swells measured in the in the near shore regions of eastern Arabian Sea, International J. Naval Architecture and Ocean Eng., 8, 312-319, doi: 10.1016/j.ijnaoe.2016.03.008, 2016.

Glejin, J., Sanil Kumar, V., Nair, B., and Singh, J.: Influence of winds on temporally varying short and long period gravity waves in the near shore regions of the eastern Arabian Sea, Ocean Science, 9 (2), 343-353, 2013.

Goda, Y.: Numerical experiments on wave statistics with spectral simulation, Report Port and Harbour Research Institute, Japan, 9, 3–57, 1970.

Gowthaman, R., Sanil Kumar V., Dwarakish, G. S., Soumya S. M, Jai Singh, and Ashok Kumar, K.: Waves in Gulf of Mannar and Palk Bay around Dhanushkodi, Tamil Nadu, India, Current Science, 104(10), 1431-1435, 2013.

Hanson, J. L., and Phillips, O. M.: Wind sea growth and dissipation in the open ocean, J. Phys. Oceanogr., 29, 1633-1648, 1999.

Hasselmann, S., Hasselmann, K., Allender, J. H., and Barnett, T. P.: Computations and parameterizations of the nonlinear energy transfer in a gravity-wave spectrum, Part II: parameterizations of the nonlinear energy transfer for application in wave models, J. Phys. Oceanogr., 15, 1378–1391, 1985.

Hemer, M. A., Church, J. A., and Hunter, J. R.: Variability and trends in the directional wave climate of the Southern Hemisphere, Int J. Climatol., 30(4), 475–491, 2010.

Henrique, R., Babanin, A. V., Schulz, E., Hemer, M. A., and Durrant, T. H.: Observation of wind-waves from a moored buoy in the Southern Ocean, Ocean Dynamics, 65, 1275-1288, 2015.

Hwang, P. A., Garcıa-Nava, H., and Ocampo-Torres, F. J.: Dimensionally consistent similarity relation of ocean surface friction coefficient in mixed seas, J. Phys. Oceanogr., 41, 1227–1238, 2011.

IMD.: Deep Depression over the Bay of Bengal (08-10 November 2015): A Report, Cyclone Warning Division, India Meteorological Department, New Delhi, http://www.rsmcnewdelhi.imd.gov.in/images/pdf/publications/preliminary-report/DD_08112015.pdf (accessed on 10 December 2016), 2015.

Johnson, G., Sanil Kumar, V. and Balakrishnan Nair, T. M.: Monsoon and cyclone induced wave climate over the near shore waters off Puduchery, south western Bay of Bengal, Ocean Eng., 72, 277–286. doi:10.1016/j.oceaneng.2013.07.013, 2013.

Kuik, A. J., Vledder, G. P., and Holthuijsen, L. H.: A method for the routine analysis of pitch and roll buoy wave data, J. Phys. Oceanogr., 18, 1020-1034, 1988.

Longuet-Higgins, M.S.: Eulerian and Lagrangian aspects of surface waves. J. Fluid Mech. 173, 683–707, 1986.

Lygre, A., and Krogstad, H. E.: Maximum entropy estimation of the directional distribution in ocean wave spectra, J. Phys. Oceanogr., 16(12), 2052–2060, 1986.

McComb, P., Johnson, D., and Beamsley, B.: Numerical model study to reduce swell and long wave penetration to Port Geraldton, Proceedings of the 2009 Pacific Coasts and Ports Conference, Wellington, New Zealand, 2009.

Nayak, S., Bhaskaran, P. K., Venkatesan, R., and Dasgupta, S.: Modulation of local wind waves at Kalpakkam from remote forcing effects of Southern Ocean swells, Ocean Engg., 64, 23-35, 2013.

Patra, A., and Bhaskaran, P. K.: Temporal variability in wind-wave climate and its validation with ESSO NIOT wave atlas for the head Bay of Bengal. Clim. Dyn., 1-18, doi:10.1007/s00382-016-3385-z,2016

Patra, S. K., Mishra, P., Mohanty, P. K., Pradhan, U. K., Panda, U. S., Ramana Murthy, M. V., Sanil Kumar, V., and Balakrishnan Nair, T. M.: Cyclone and monsoonal wave characteristics of northwestern Bay of Bengal: long-term observations and modeling, Natural Hazards, 82,1051–1073, doi:10.1007/s11069-016-2233-0, 2016.

Portilla. J., Ocampo-Torres, F. J., and Monbaliu, J.: Spectral Partitioning and Identification of Wind Sea and Swell, J. Atmos. Oceanic Technol., 26, 107-122, 2009.

Sanil Kumar, V., Anand, N. M., Kumar, K. A., and Mandal, S.: Multipeakedness and groupiness of shallow water waves along Indian coast, J. Coastal Res., 19, 1052-1065, 2003.

Sanil Kumar, V., Glejin J., Dora, G. U., Sajiv, P. C., Singh, T., and Pednekar, P.: Variations in near shore waves along Karnataka, west coast of India, J. Earth System Science, 121, 393-403. doi:10.1007/s12040-012-0160-3, 2012.

Sanil Kumar, V., Dubhashi, K. K., Balakrishnan Nair, T. B., and Singh, J.: Wave power potential at few shallow water locations around Indian coast, Current Science, 104(9), 1219-1224, 2013.

Sanil Kumar, V., Dubhashi, K. K. and Nair, T. B.: Spectral wave characteristics off Gangavaram, Bay of Bengal, J. Oceanography, 70(3):307-321, doi:10.1007/s10872-014-0223-y, 2014.

Sanil Kumar, V., Shanas, P. R., and Dubhashi, K. K.: Shallow water wave spectral characteristics along the eastern Arabian Sea, Natural Hazards, 70, 377–394, doi:10.1007/s11069-013-0815-7, 2014.

Sundar, V.: Wave characteristics off the South East Coast of India, Ocean Engg., 13(4), 327-338, 1986.

Thompson, W. C., Nelson, A. R., and Sedivy, D. G.: Wave group anatomy of ocean wave spectra, Proceeding of 19th conference on Coastal engineering, American Society of Civil Engineers, 1, 661–677, 1984.

Toffoli, A., Onorato, M., and Monbaliu, J.: Wave statistics in unimodal and bimodal seas from a second-order model, European Journal of Mechanics B/Fluids, 25, 649–661, 2006.

Tolman, H. L.: A third-generation model for wind waves on slowly varying, unsteady, and inhomogeneous depths and currents, J. Phys. Oceanogr., 21, 782–797, 1991.

USACE: Shore Protection Manual, Department of the Army, U.S. Corps of Engineers, Washington, DC, 3-81 to 3-84, 1984.

Whittaker, C. N., Raby, A. C., Fitzgerald, C. J., and Taylor, P. H.: The average shape of large waves in the coastal zone, Coastal Engg., 114, 253–264, 2016.

Wyrtki, K.: Oceanographic atlas of the international Indian Ocean expedition. Washington, DC: ,National Science Foundation, 1971.

Young, I. R., Zieger, S., and Babanin, A. V: Global trends in wind speed and wave height, Science. 332(6028), 451–455, 2011.

Table 1. Studies on waves in Indian waters based on measured wave data covering 1 year and above

Location	Position	Water depth (m)	Period of data used	Aspects studied	Reference
Ratnagiri, eastern Arabian Sea	16.980˚ N; 73.258˚ E	13	1 January 2011-31 December 2011	Short-term statistics of waves	Amrutha and Sanil Kumar (2014)
			1 May 2010-30 April 2012	Seasonal and annual variations in waves, role of sea breeze and land breeze on waves	Glejin et al. (2013)
Eastern Arabian Sea	16.980° N; 73.258° E	13	1 January 2011-31 December 2012	Characteristics of long-period swells	Glejin et al. (2017)
	14.822° N, 74.052° E	15			
	14.304° N; 74.391° E	9			
Honnavar, eastern Arabian Sea	14.304° N, 74.414° E	5	22 April 2011-17 December 2011	Seasonal variation in wave characteristics and spatial and temporal variations of wave energy	Amrutha and Sanil Kumar (2017)
			1 June 2015-31 July 2015		
	14.304° N, 74.391° E	9	1 January		

	14.307° N, 74.291° E	30	2009-31 December 2015 18 April 2014-18 August 2014 1 June 2015-31 July 2015		
Off Dhanushkodi, Gulf of Mannar	9.113° N; 79.407° E	12	9 February 2010-31 March 2011	Seasonal variations in wave characteristics and wave spectra	Gowthaman et al. (2013)
Off Dhanushkodi, Pal Bay	9.319°N; 79.434°E	12	9 February 2010-31 March 2011	Seasonal variations in wave characteristics and wave spectra	Gowthaman et al. (2013)
Puducherry, western Bay of Bengal	11.924° N : 79.851° E	15	1 January 2009-29 December 2011	Seasonal and annual variations in monsoon and cyclone induced waves. Influence of sea and land breeze on waves	Johnson et al. (2013)
Gangavaram, western Bay of Bengal	17.633° N 83.267° E	18	1 January 2010- 31 December 2010	Spectral wave characteristics and seasonal variations	Sanil Kumar et al. (2014)
Gopalpur, northern Bay of Bengal	19.258°N 84.907°E	23	1 June 2008-31 May 2009	Variations in wind-sea and swell characteristics	Patra et al. (2016)

Table 2. Statistics of each month: mean value, standard deviation, maximum and minimum of significant wave height along with swell and wind-sea percentage in the measured data

Month	Mean (m)	Standard deviation (m)	Maximum (m)	Minimum (m)	No. of data	Swell (%)	Wind-sea (%)
May 2015	0.91	0.22	1.69	0.46	1488	54.3	45.7
June 2015	1.08	0.19	1.70	0.70	1439	58.0	42.0
July 2015	0.88	0.12	1.54	0.61	1488	64.5	35.5
August 2015	0.93	0.17	1.57	0.60	1488	63.9	36.1
September 2015	1.01	0.19	1.56	0.55	1438	58.8	41.2
October 2015	0.82	0.20	1.53	0.34	1488	63.3	36.7
November 2015	0.70	0.13	1.19	0.34	1439	59.8	40.2
December 2015	0.72	0.17	1.21	0.35	1488	30.7	69.3
January 2016	0.75	0.15	1.27	0.36	1484	28.9	71.1
February 2016	0.75	0.16	1.15	0.42	1389	38.0	62.0
March 2016	0.75	0.16	1.31	0.43	1488	53.6	46.4
April 2016	0.78	0.17	1.34	0.37	1440	60.1	39.9
Annual average	0.84	0.21	1.70*	0.34*	1463	52.8	47.2

*extremes

Table 3. Average wave parameters and number of data in different spectral peak frequencies

Peak frequency (f_p) range (Hz)	Number of data and %	H_{m0} (m)	T_{m02} (s)	Peak wave period (s)
$0.04 < f_p \leq 0.05$	139 (0.79)	0.91	4.98	20.14
$0.05 < f_p \leq 0.06$	1573 (8.96)	0.91	5.17	17.13
$0.06 < f_p \leq 0.07$	3838 (21.86)	0.85	4.97	14.71
$0.07 < f_p \leq 0.08$	4429 (25.23)	0.80	4.80	12.96
$0.08 < f_p \leq 0.10$	4921 (28.03)	0.82	4.71	11.06
$0.10 < f_p \leq 0.15$	368 (2.10)	0.80	4.50	8.69
$0.15 < f_p \leq 0.20$	477 (2.72)	1.05	4.03	5.30
$0.20 < f_p \leq 0.30$	1779 (10.13)	0.86	3.65	4.32
$0.30 < f_p \leq 0.50$	33 (0.19)	0.73	3.33	3.23

Table 4. Percentage of single-peaked and multi-peaked wave spectra in different months along with spectral peak period (wind-sea, swell or mixed)

Month	Single-peak (%)				Multi-peak (%)			
	Total	Wind-sea (T_p<6)	Swell (T_p>8)	Mixed (6 <T_p< 8)	Total	Wind-sea dominated (T_p<6)	Swell dominated (T_p>8)	Mixed (6 <T_p<8)
May	40.2	0.8	39.4	0	59.8	9.7	45.6	4.6
June	55.8	0.1	55.7	0	44.2	1.7	42.1	0.4
July	57.8	0.0	57.8	0	42.2	1.1	41.1	0.0
August	48.3	0.0	48.3	0	51.7	3.3	48.4	0.0
September	51.3	0.1	51.2	0	48.7	5.6	43.0	0.2
October	48.0	0.1	47.9	0	52.0	4.2	46.9	0.9
November	47.0	0.0	47.0	0	53.0	3.3	49.8	0.0
December	15.0	0.5	14.4	0	85.0	34.2	50.8	0.0
January	9.5	0.5	9.0	0	90.5	31.4	59.1	0.0
February	25.1	0.3	24.8	0	74.9	27.5	47.4	0.0
March	43.3	0.0	43.3	0	56.7	21.8	34.8	0.0
April	56.5	0.1	56.5	0	43.5	8.5	35.0	0.0
Annual average	41.5	0.2	41.3	0.0	58.5	12.7	45.3	0.5

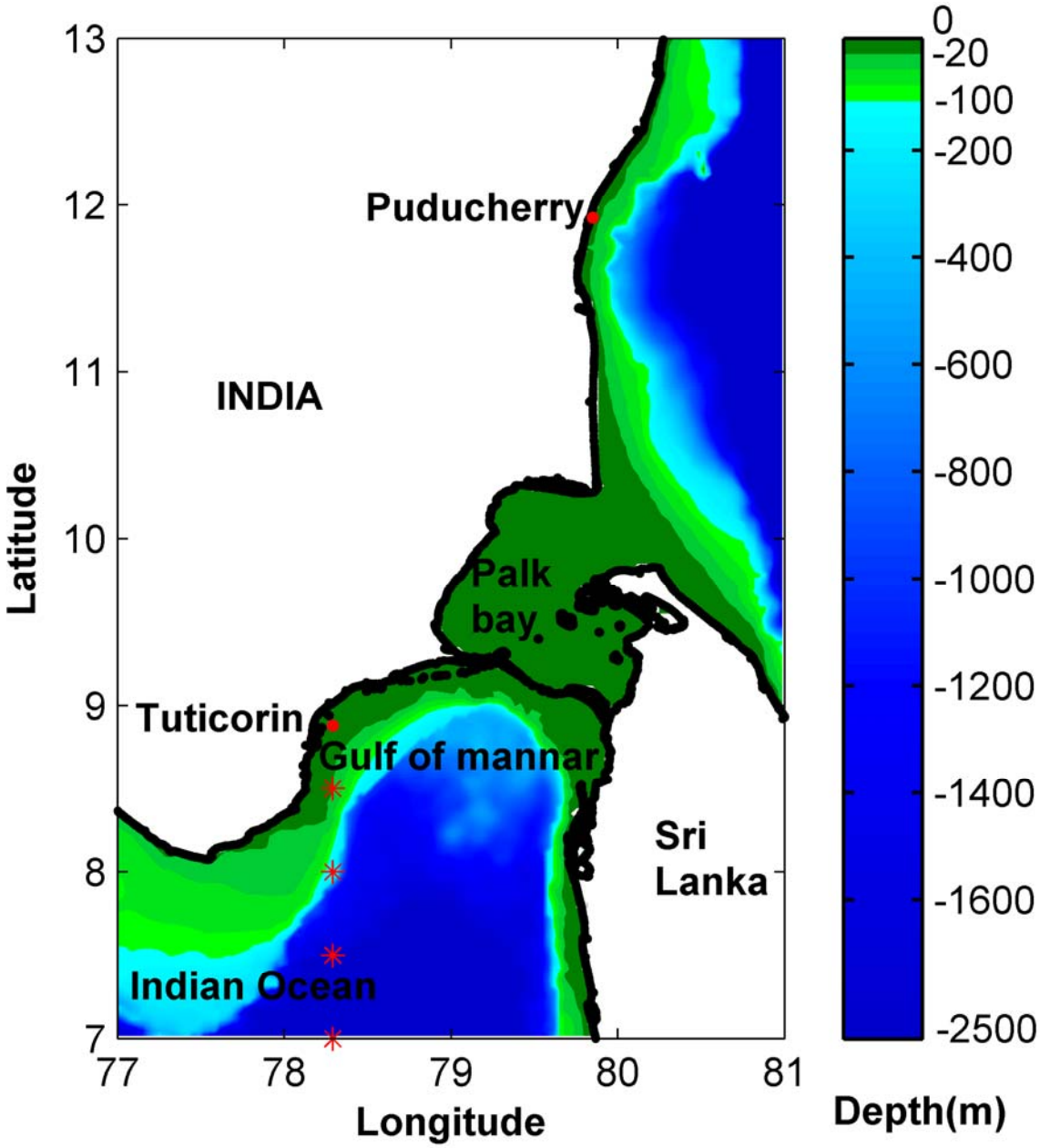

Figure 1. The location of the waverider buoy mooring in the region of interest in the Gulf of Mannar. The bathymetry is from ETOPO1, 1 Arc-Minute Global Relief Model (Amante and Eakins, 2009). The star symbol indicates the points considered for studying the percentage change in swells.

a) February-May

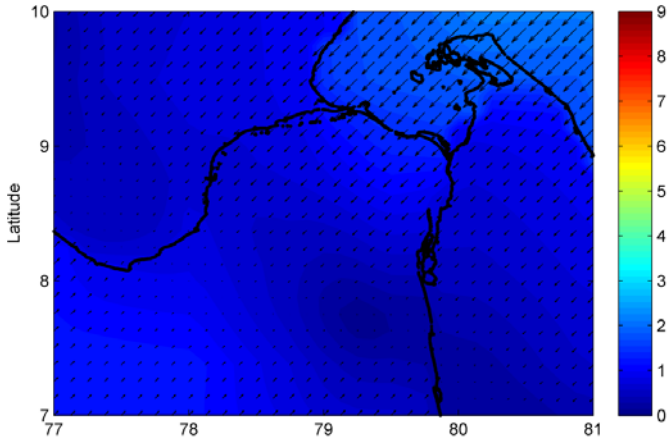

b) June-September

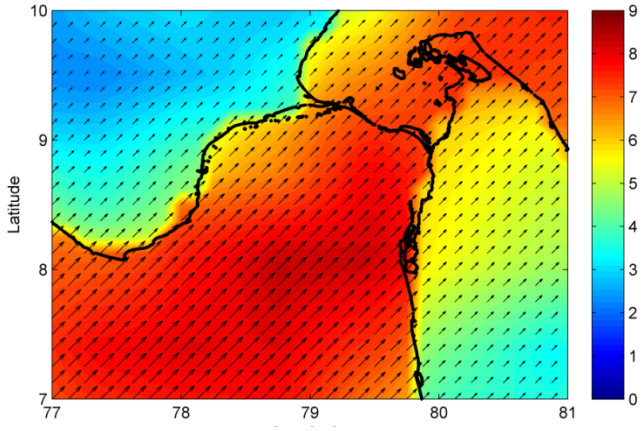

c) October-January

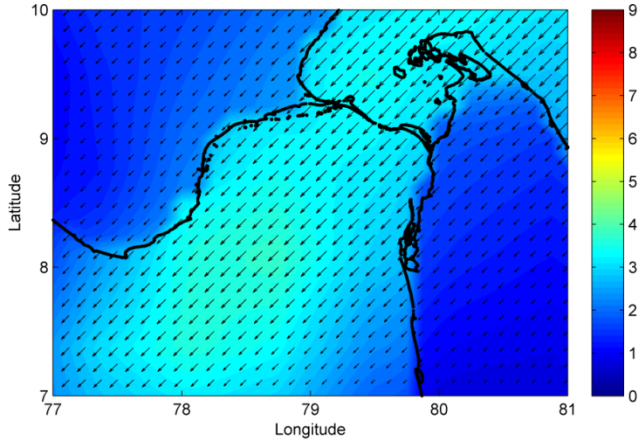

Figure 2. Wind field over the study area in different seasons; a) pre-monsoon (February-May), b) southwest monsoon (June-September) and c) northeast monsoon (October-January). Wind field is from ERA-Interim reanalysis data and the wind speed is in m s^{-1}

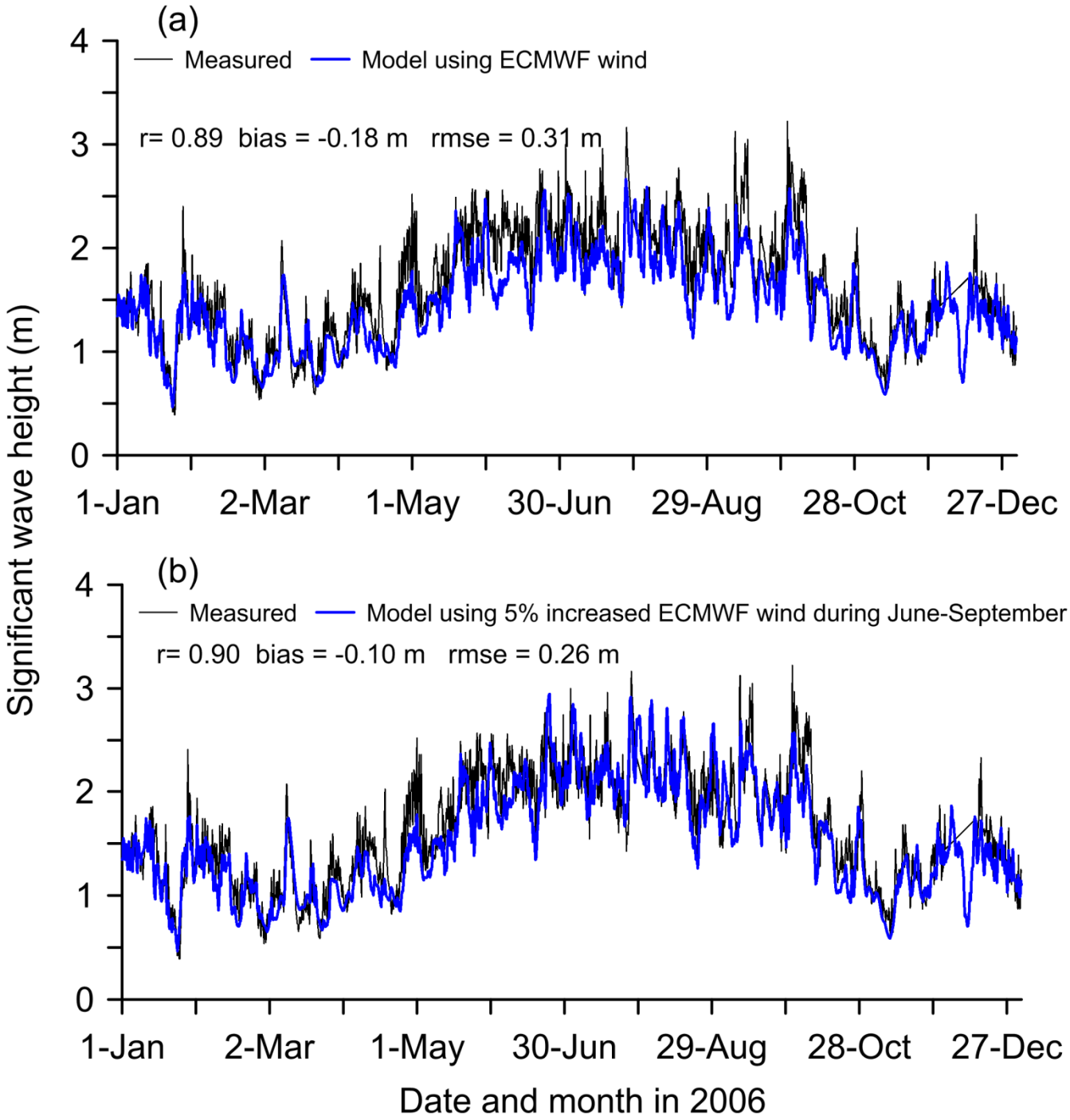

Figure 3. Time history of simulated significant wave height through numerical model forced by (a) ECMWF wind and (b) ECMWF wind speed increased by 5% during June-September and its comparison with field measurements at 8.27^{o} N, 78.56^{o} E during January-December 2006.

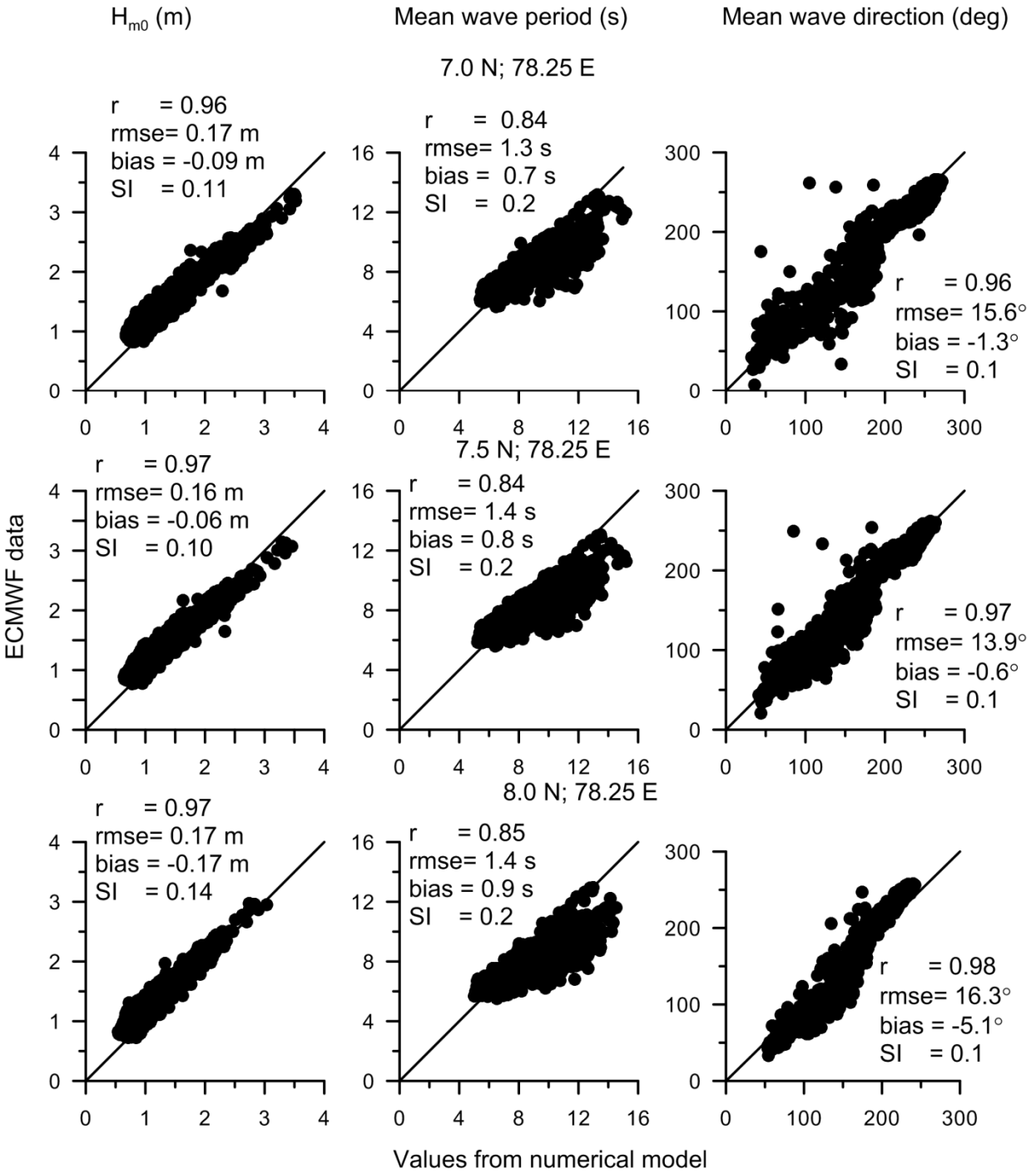

Figure 4. Correlation between model data with ECMWF ERA-Interim data of significant wave height, mean wave period and mean wave direction at different locations

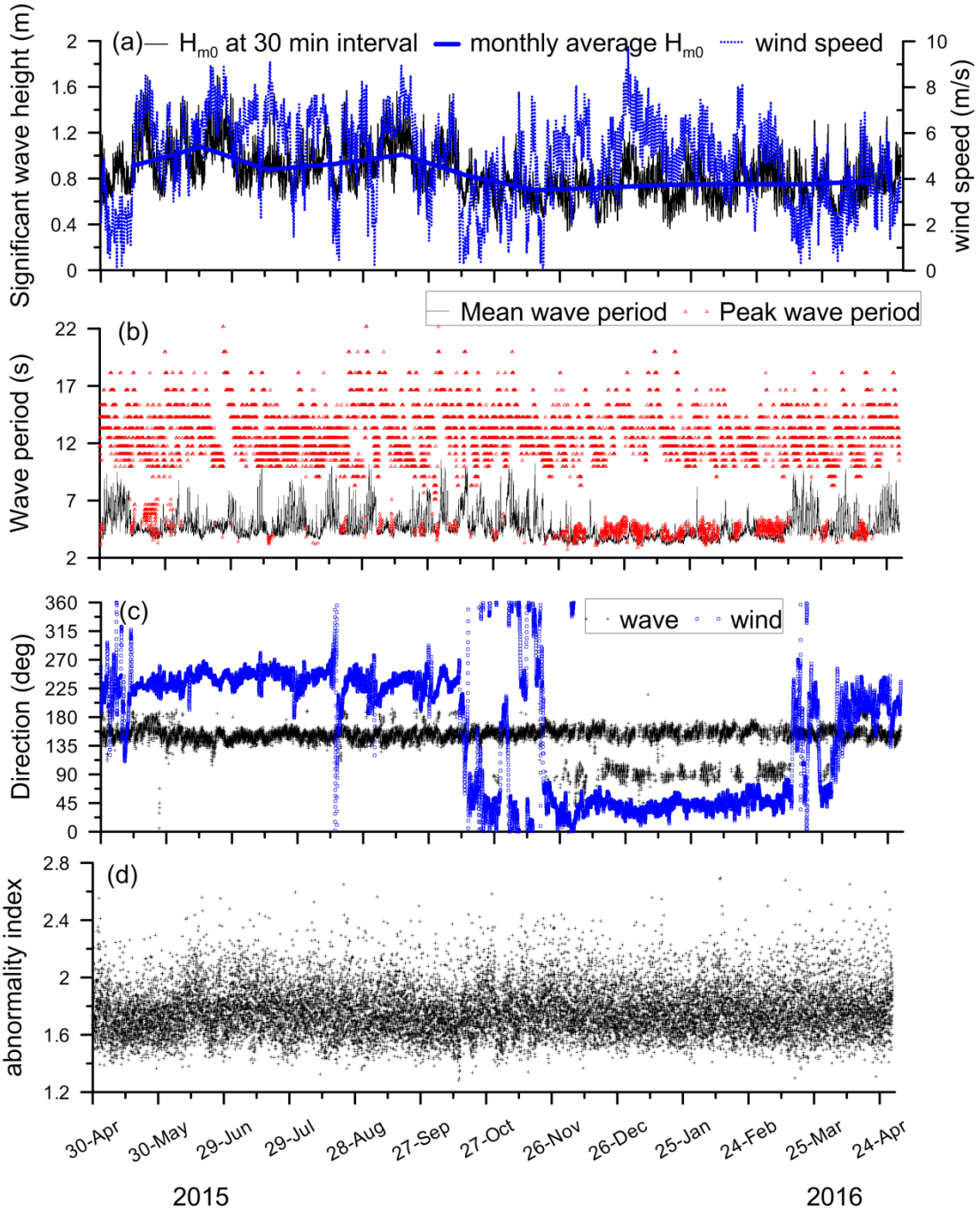

Figure 5. Time series plots of (a) significant wave height and wind speed, (b) mean wave period for data covering 30 minutes and peak wave period, (c) direction of wind and wave and (d) abnormality index. The monthly average significant wave height values are also shown

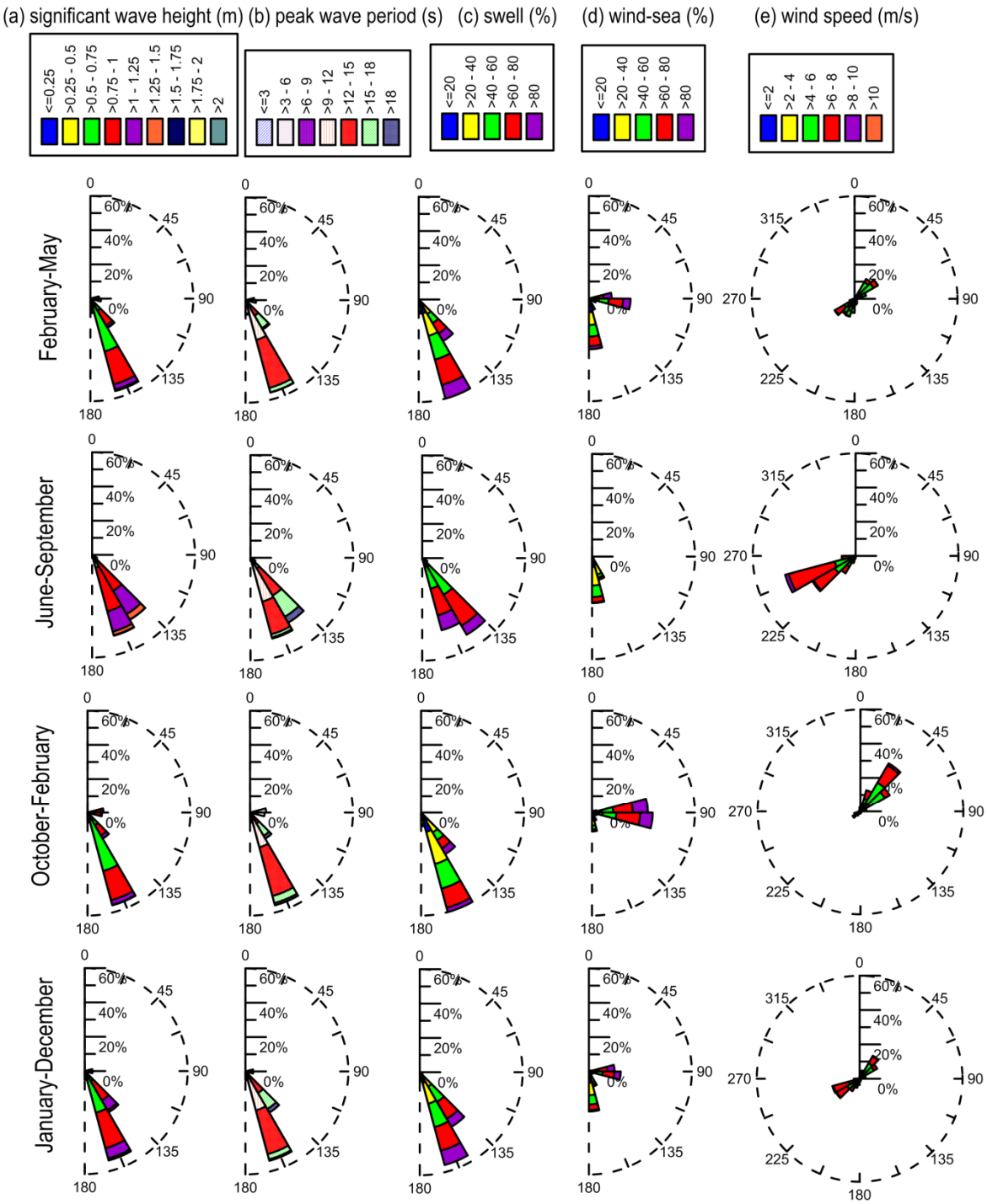

Figure 6. Wave roses during 1 May 2015 to 30 April 2016 (a) significant wave height and mean wave direction, (b) peak wave period and mean wave direction, (c) percentage of swell in the measured data and mean wave direction, (d) percentage of wind-sea in the measured data and mean wave direction, (e) wind speed and direction. The plots represent the direction where the waves come from. The radius of the figure indicates the percentage of the time.

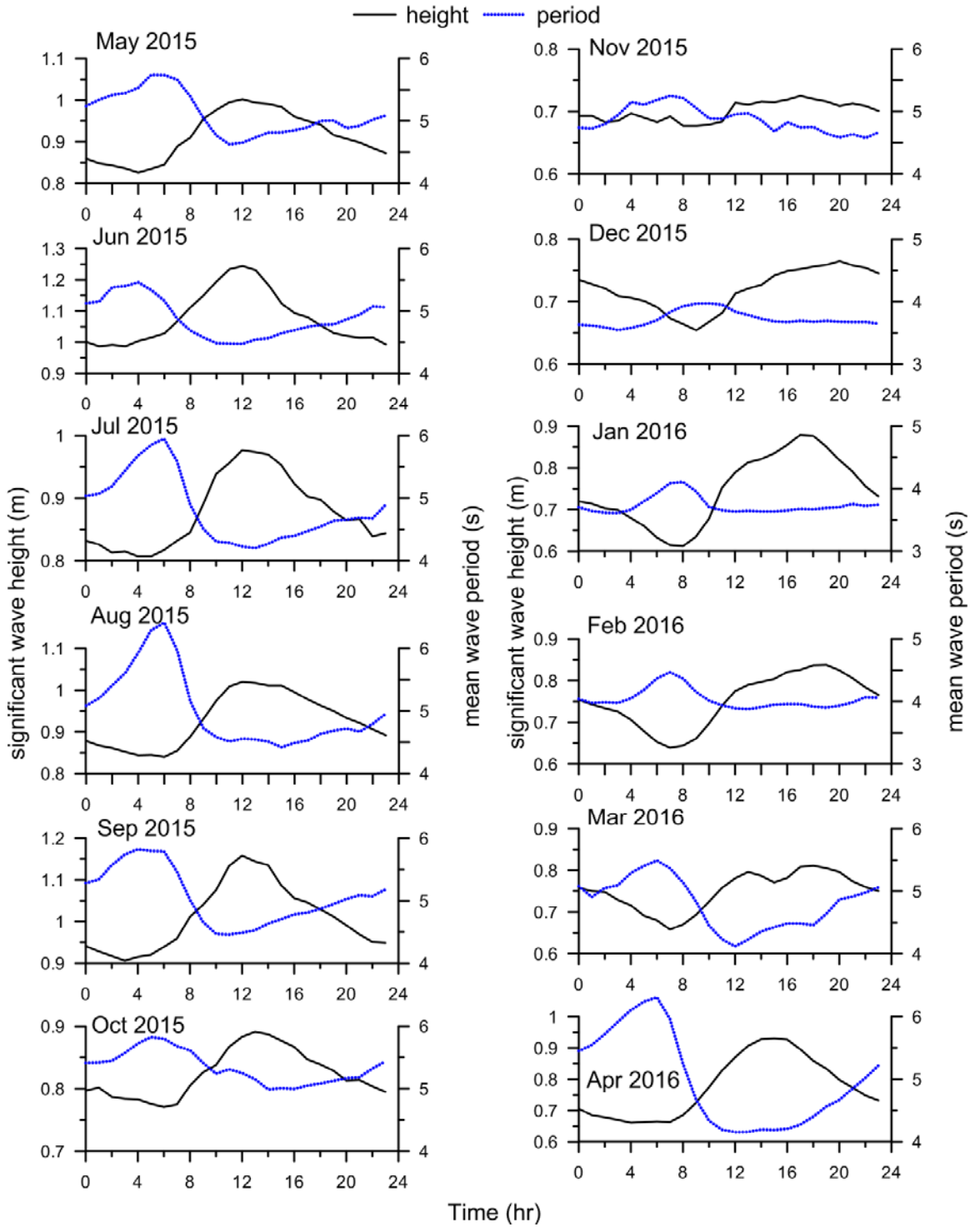

Figure 7. Variation of hourly averaged significant wave height and mean wave period in different months

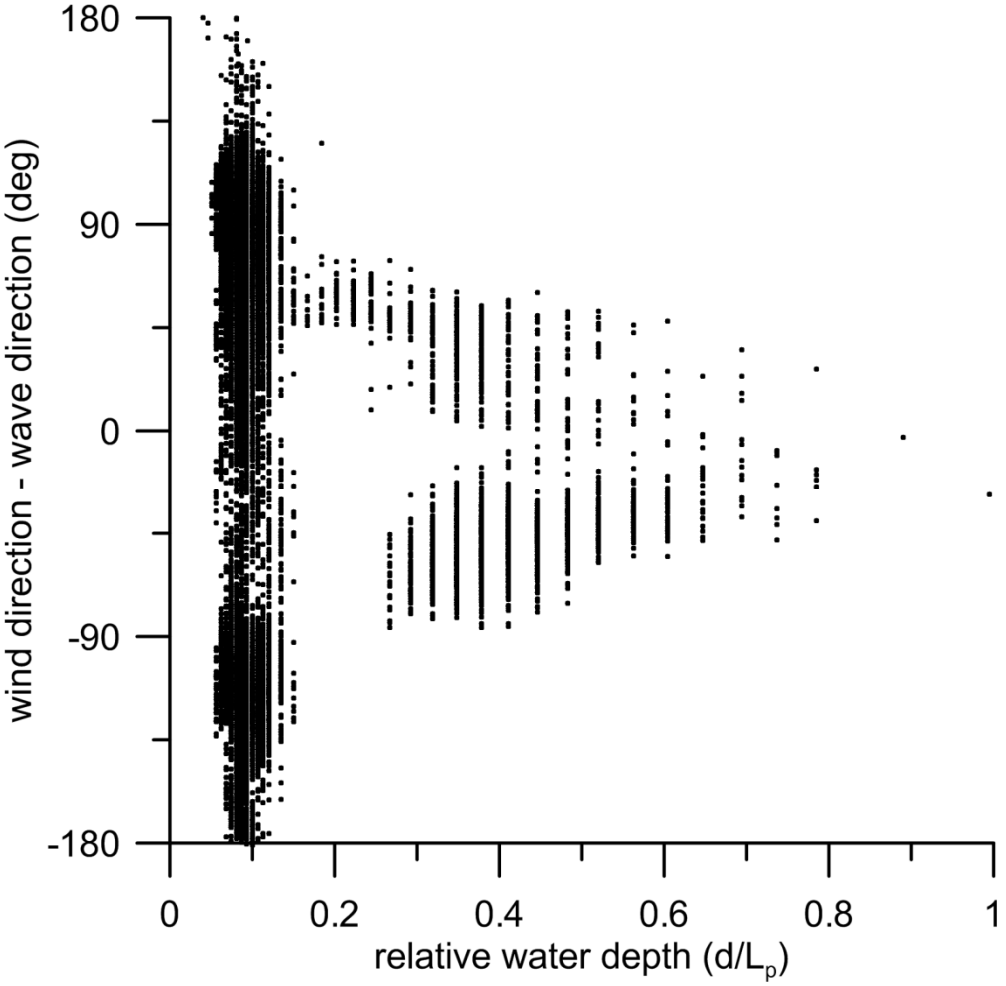

Figure 8. Variation of difference in wind and wave direction with relative water depth

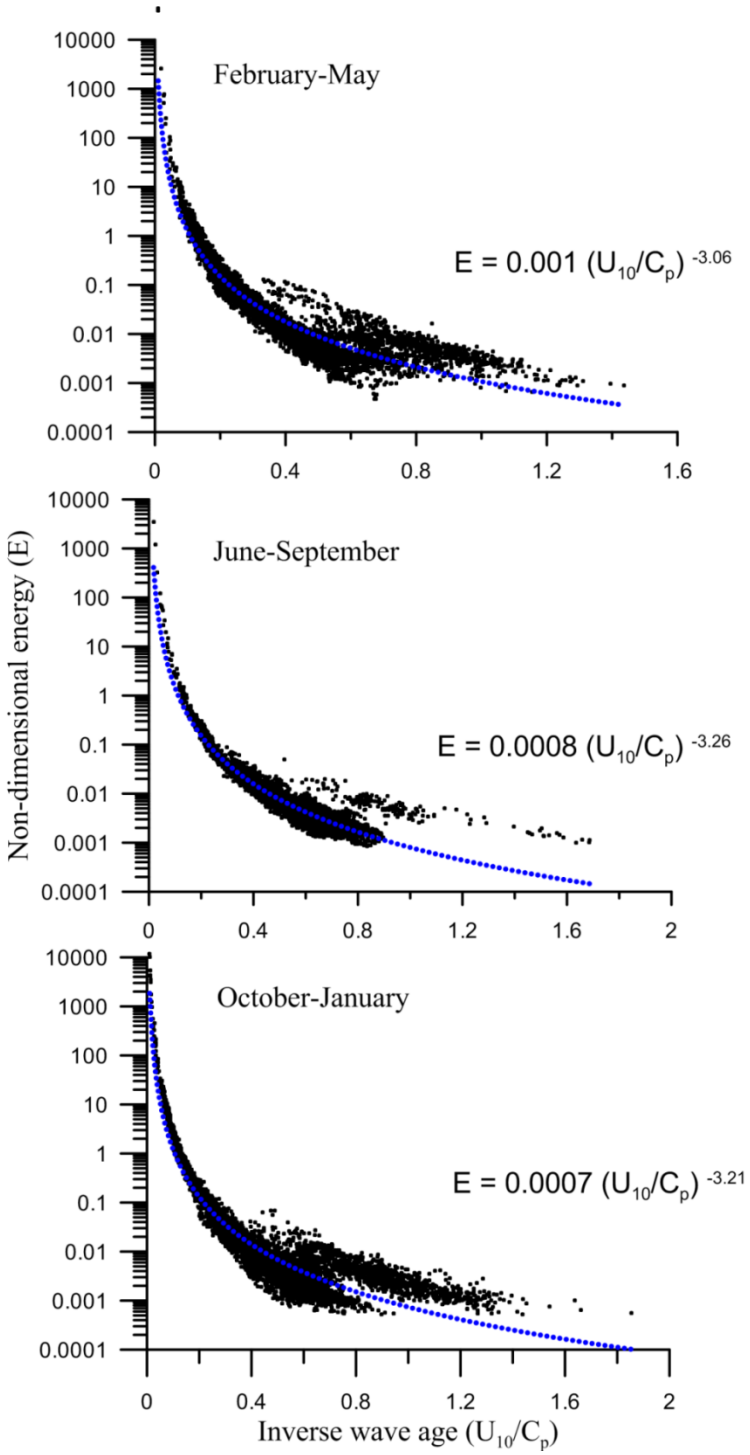

Figure 9. Variation of non-dimensional energy with inverse wave age in different periods; a) February-May, b) June-September, c) October-January

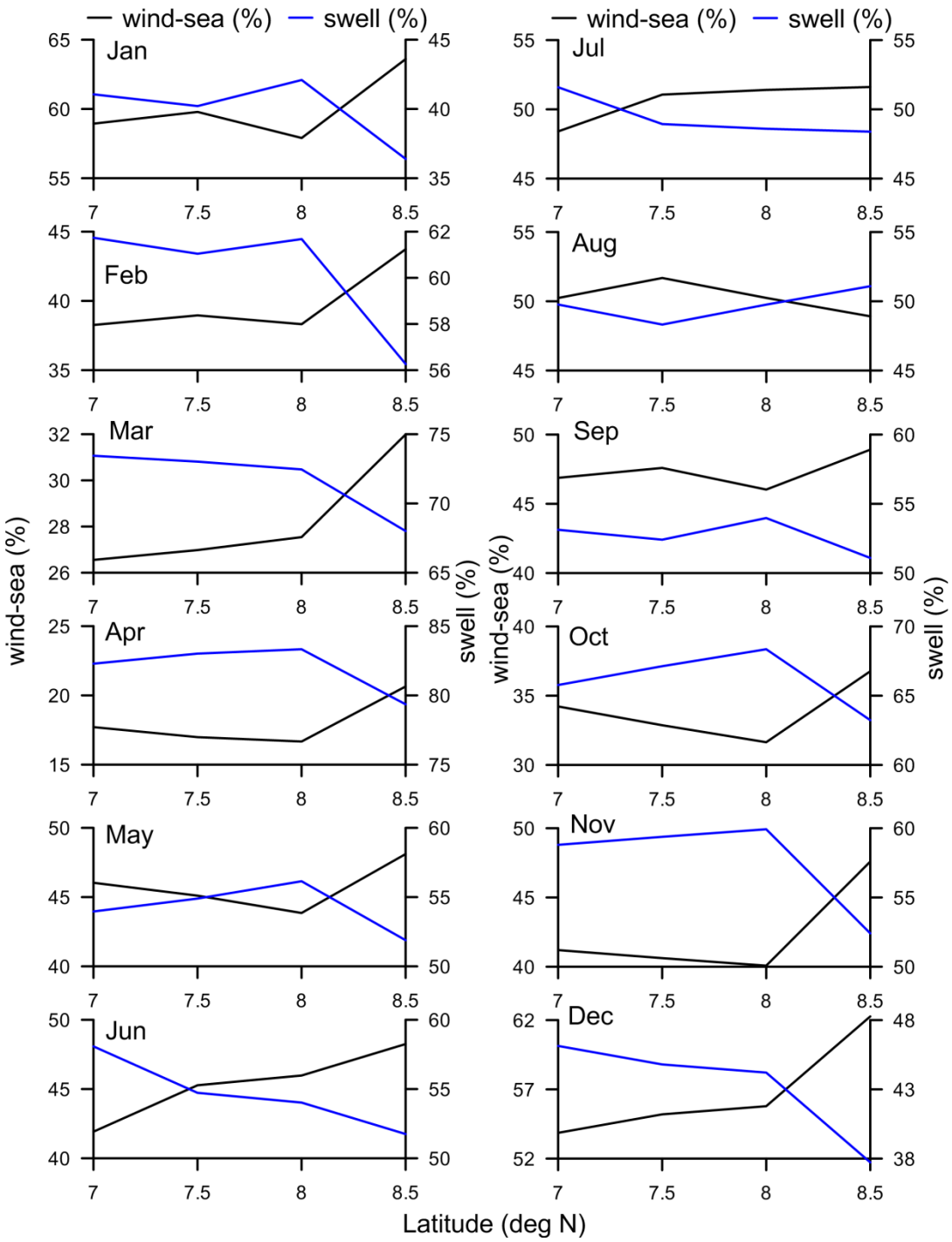

Figure 10. Swell and wind-sea percentage at 7, 7.5, 8 and 8.5° N latitude in different months based on wave model results

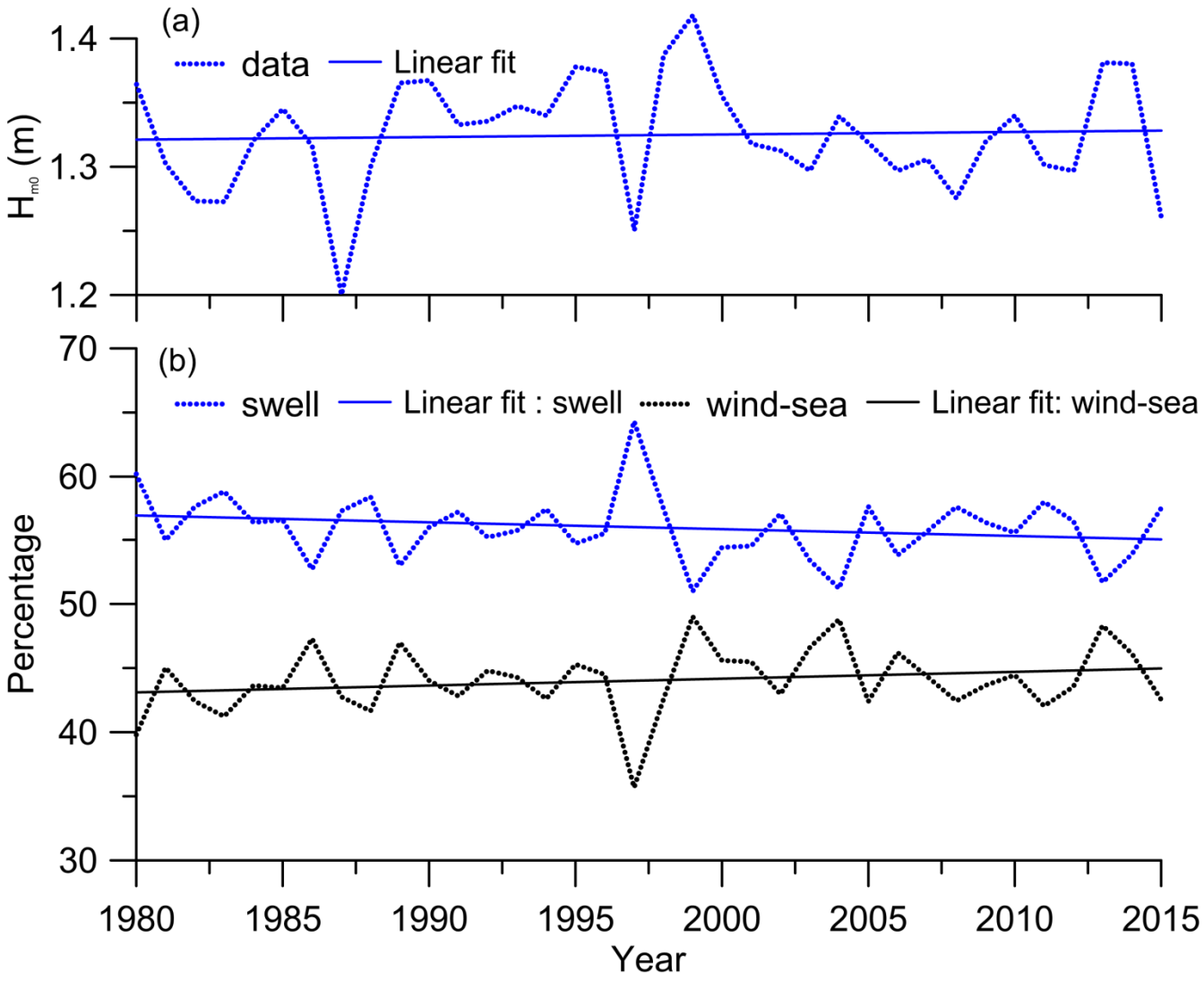

Figure 11. Variation in a) significant wave height and b) percentage swell and wind-sea at 8° N; 78.29° E during 1980-2015. Linear trend is also presented.

5

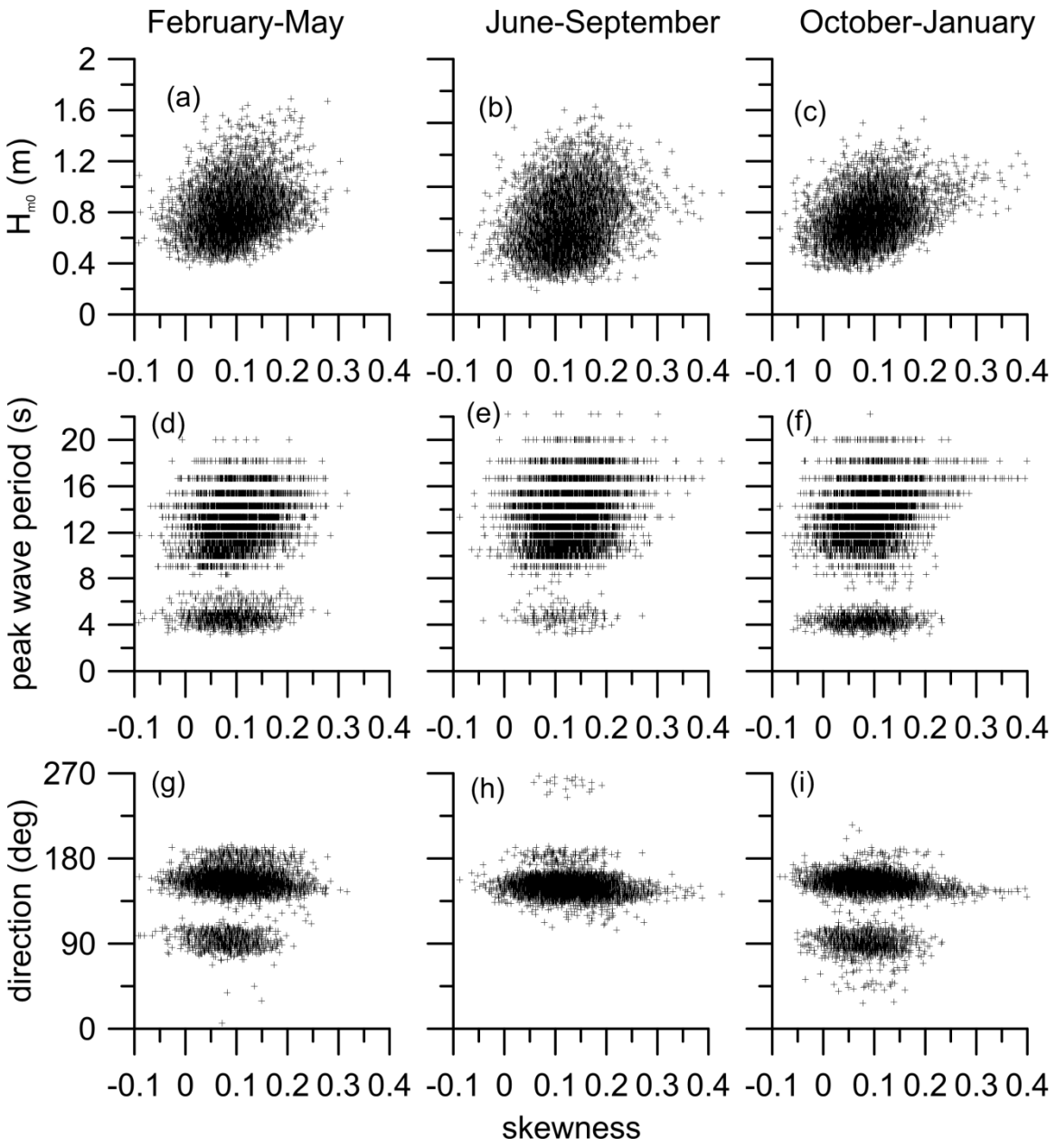

Figure 12. Variation of skewness with significant wave height, mean wave period and mean wave direction in different seasons

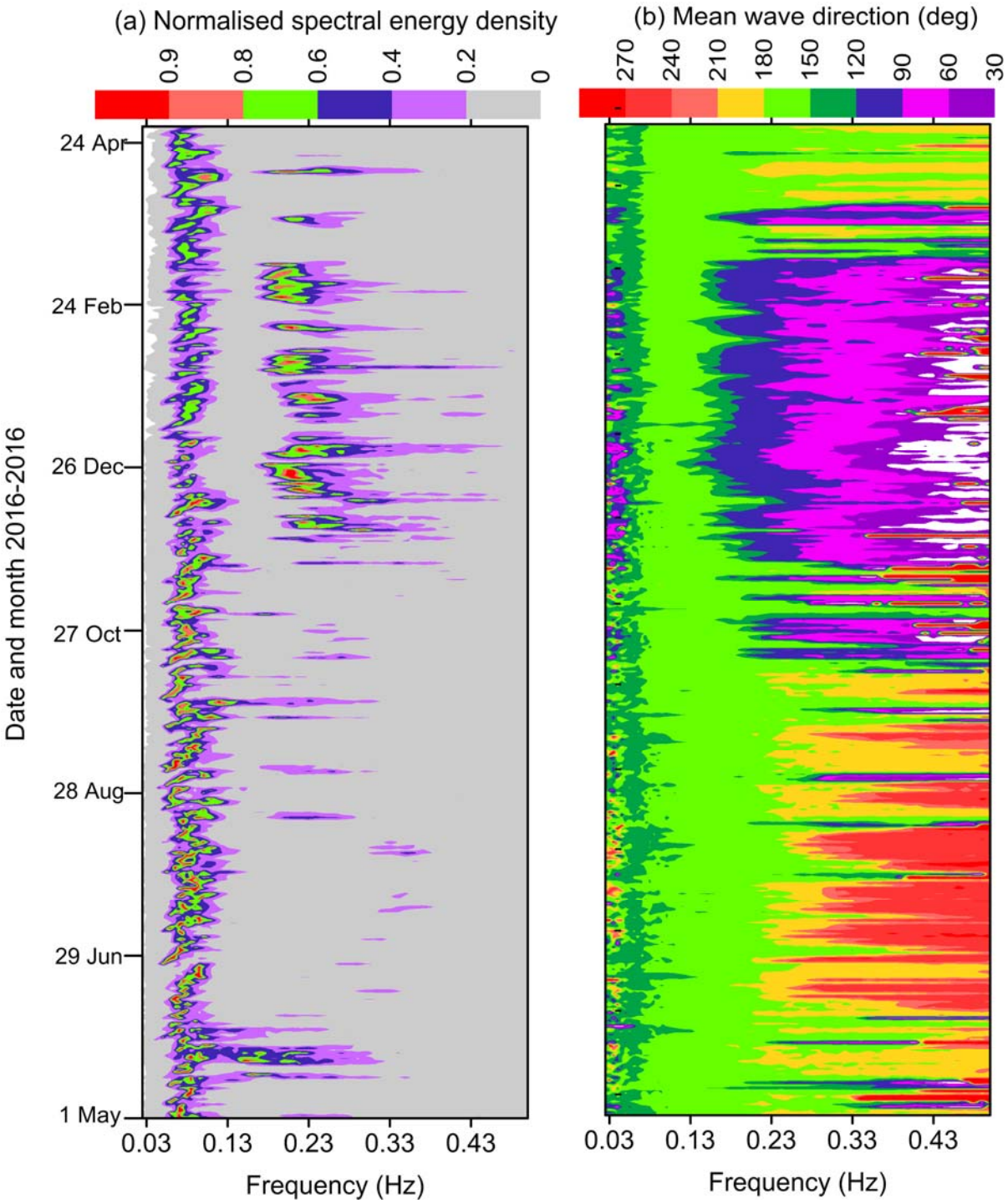

Figure 13. Contour plots of (a) normalized spectral energy density and (b) mean wave direction during 1 May 2015 to 30 April 2016

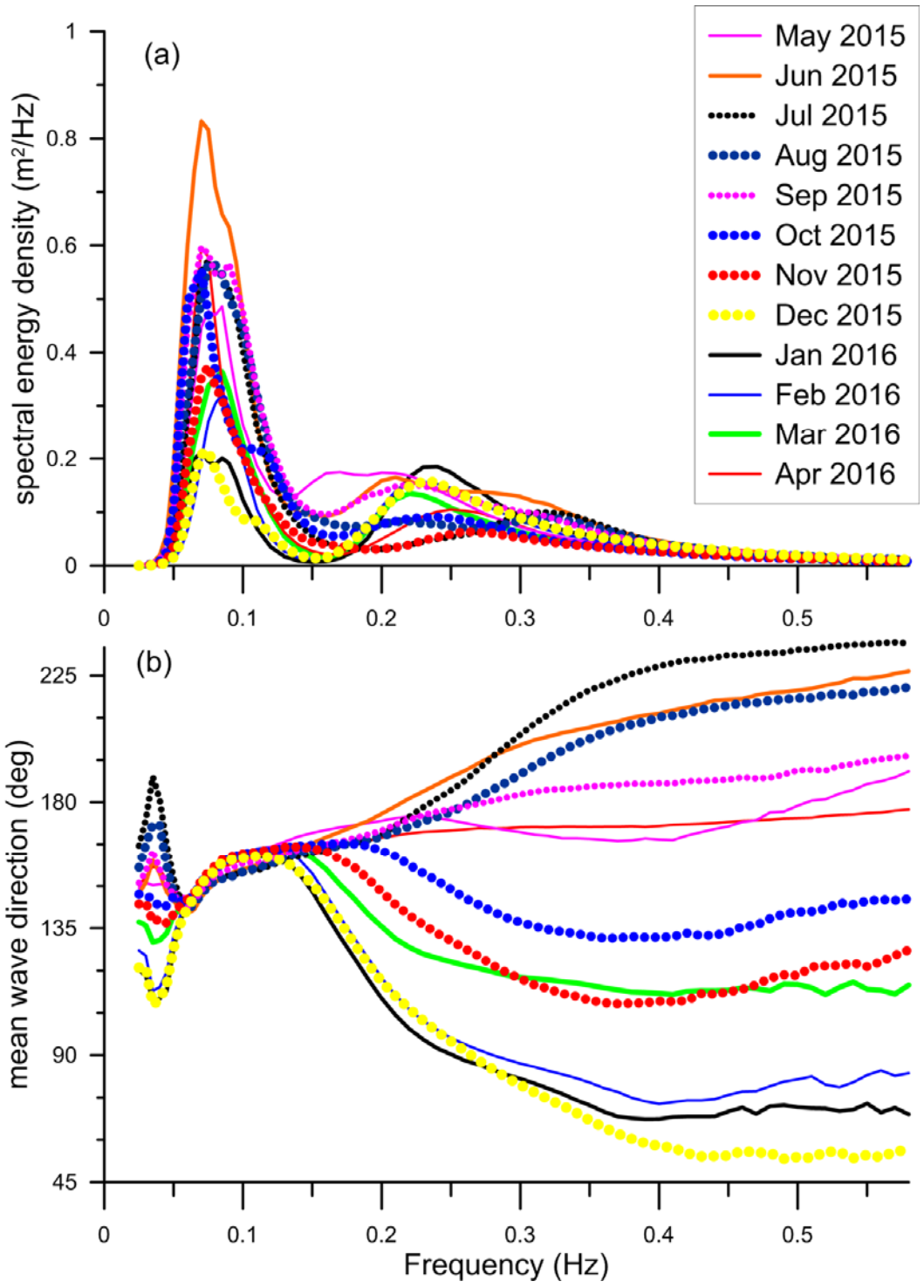

Figure 14. Monthly average wave spectrum (a) and mean wave direction (b) during May 2015 to April 2016

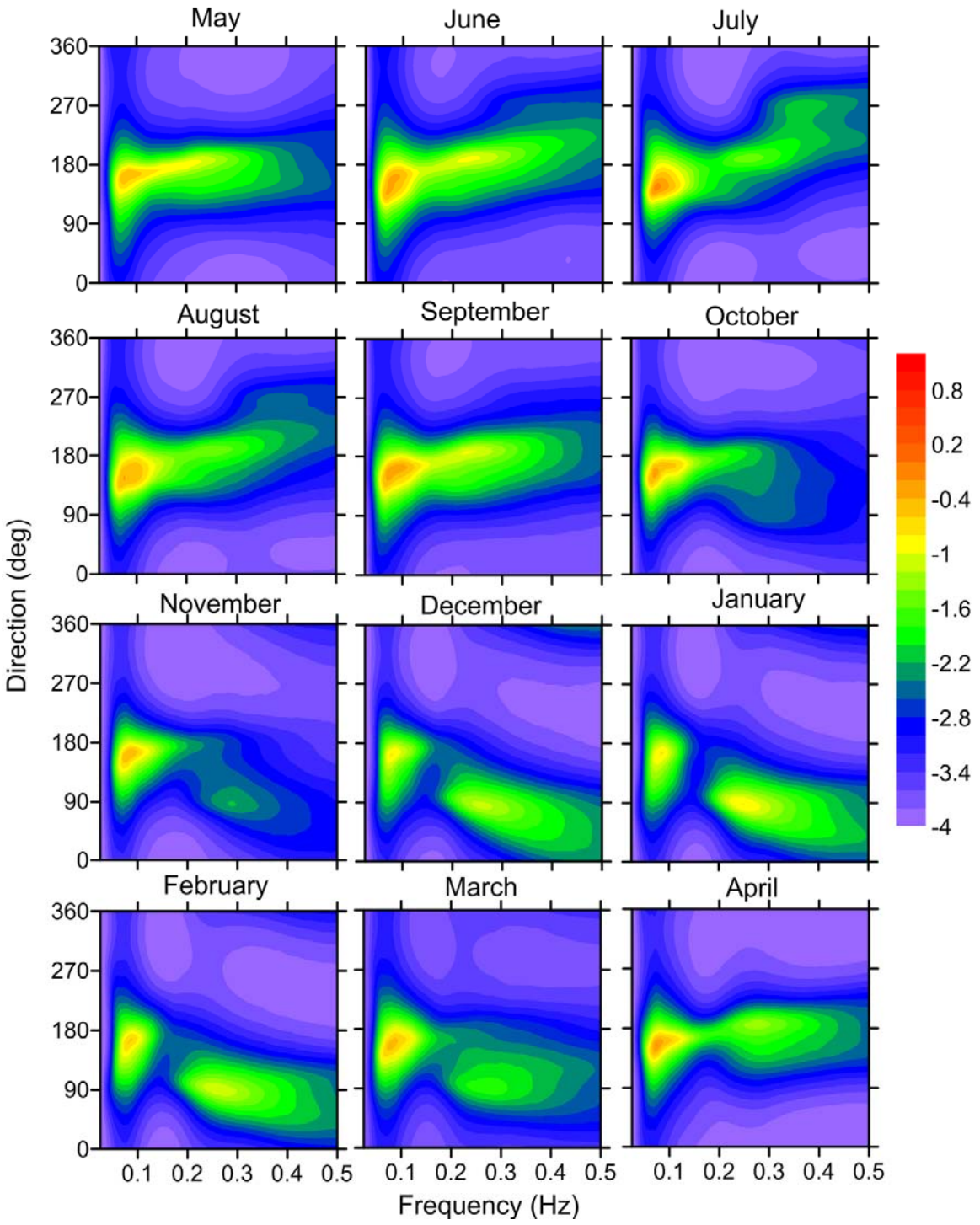

Figure 15. Monthly average directional wave spectrum during different month. The color bar is for spectral energy (m^2 /Deg/Hz) . The spectral energy is shown in logarithmic scale (base 10).

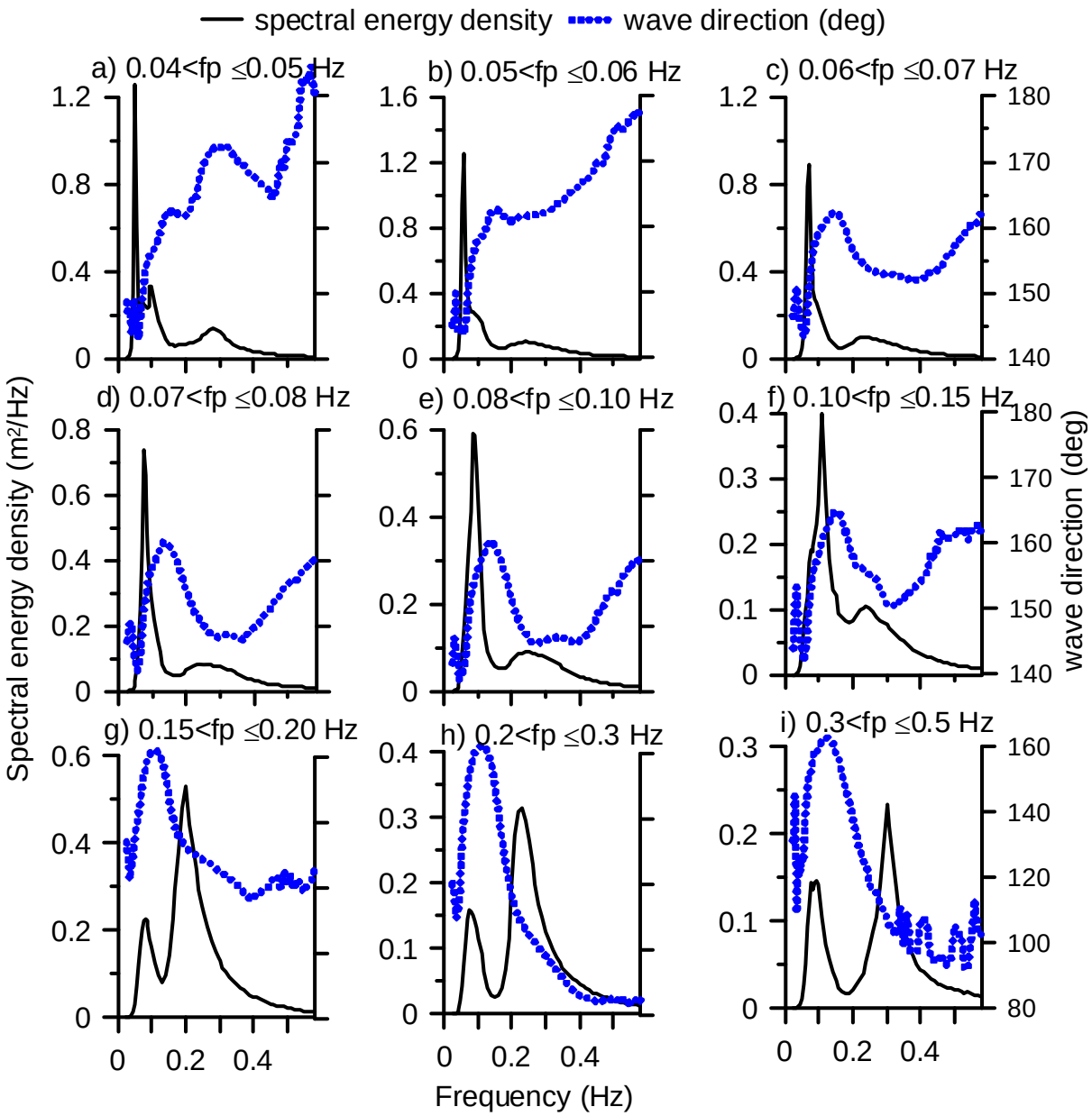

Figure 16. Plot of average spectral energy density and average mean wave direction of waves grouped under different peak frequency bins